Mathematical Models for Dry Wear of H18 Heat Treated AA1100/TiB_2 Composites

[1]V. K. Reddy and A. Chennakesava Reddy[2]

[1]Research Scholar, Department of Mechanical Engineering, JNTU College of Engineering, Hyderabad, India
[2]Professor, Department of Mechanical Engineering, JNTU College of Engineering, Hyderabad, India

Abstract: *In the present work, the AA1100-TiB_2 metal matrix composites were manufactured at 10% and 30% volume fractions of TiB_2. The composites were wear tested at different levels of normal load, sliding speed and sliding distances. The microstructure of worn surfaces pertaining to AA1100 alloy/ TiB_2 composite reveals the detachment of TiB_2 particles from the matrix. Power-law relationships were correlated with the results obtained from the Taguchi's design of experimentation.*

Keywords: *Metal matrix composite, AA1100 alloy, titanium boride, wear, sliding distance, normal load, sliding speed.*

1. INTRODUCTION

The aluminum-alloy-based metal matrix composites reinforced with ceramic particles are widely used in aerospace, military, and civil manufacturing industries, because of their high strength, modulus, wear resistance and fatigue resistance. The surface properties dictate the life span of components in several applications. A combination of high surface wear resistance and high toughness of the interior bulk material is required to prolong the life span [1-20]. In searching the literature for models and equations, over 300 equations were found for friction and wear. The controlling of wear should be considered cautiously on the basis of selecting the alloy composition, reinforcement and also the processing methods. The effect of process parameters and the addition of reinforcement on the dry sliding wear of the composites were investigated vastly and explained that incorporation of hard secondary constituent in the matrix significantly improves the wear resistance [21-27].

The exposure on TiB_2 particles reinforced aluminum composites was not that much in the present scenario. Accordingly, the current study was focused on the exploration on dry sliding wear behavior of the AA1100/ TiB_2 composites through Taguchi's statistical model [28, 29] and developing mathematical models to compute wear.

2. MATERIALS METHODS

AA1100 alloy/ TiB_2 composites were fabricated by the stir casting process and low pressure casting technique with argon gas at 3.0 bar. The reinforcement material was titanium boride (TiB_2) nanoparticles of average size 100nm. The composite samples were given H18 heat treatment. The heat-treated samples were machined to get cylindrical specimens as per ASTM standards for the wear tests. The design of experiments for wear tests was carried out as per Taguchi techniques. The levels chosen for the controllable process parameters are summarized in Table 1. Each of the process parameters was deliberated at three levels. The orthogonal array, L9 (Table 2) was preferred to carry out experiments. A pin on disc type friction and wear monitor (ASTM G99) was employed to evaluate the friction and wear behavior of AA1100 alloy/TiB_2 composites against hardened ground steel (En32) disc.

Table 1: Control parameters and levels

Factor	Symbol	Level–1	Level–2	Level–3
Reinforcement, Vol.%	A	10	20	30
Load, N	B	20	30	40
Speed, m/s	C	2	3	4
Sliding distance, m	D	500	1000	1500

The microhardness was measured in terms of Knoop hardness number. The Knoop indenter is a diamond ground to pyramidal form that produces a diamond shaped indentation having approximate ratio between long and short diagonals of 7:1. The depth of indentation is about 1/30 of its length. When measuring the Knoop hardness, only the longest diagonal of the indentation was measured and this was used in the formula mentioned in Eq. (1) with the load used to calculate KHN. The Knoop hardness number KHN is the ratio of the load applied to the indenter, P (kgf) to the unrecovered projected area:

$$KHN = \frac{P}{CL^2} \tag{1}$$

where,
P = applied load in kgf
L = measured length of long diagonal of indentation in mm
C = 0.07028 = Constant of indenter relating projected area of the indentation to the square of the length of the long diagonal

Table 2: Orthogonal array (L9) and control parameters

Treat No.	A	B	C	D
1	1	1	1	1
2	1	2	2	2
3	1	3	3	3
4	2	1	2	3
5	2	2	3	1
6	2	3	1	2
7	3	1	3	2
8	3	2	1	3
9	3	3	2	1

The influence of sliding speed, contact time, normal pressure, and volume fraction of TiB_2 on the wear rate was estimated. Scanning electron microscopy analysis was also carried out to find consequence of wear test AA1100/ TiB_2 composite specimens.

Elastic modulus was estimated assuming the behavior of isotropic materials. The upper-bound equation is given by

$$\frac{E_c}{E_m} = \left(\frac{1-v_v^{2/3}}{1-v_v^{2/3}+v_v}\right) + \frac{1+(\delta-1)v_p^{2/3}}{1+(\delta-1)\left(v_p^{2/3}-v_p\right)} \tag{2}$$

The lower-bound equation is given by

$$\frac{E_c}{E_m} = 1 + \frac{v_p - v_p}{\delta/(\delta-1)-(v_p+v_v)^{1/3}} \tag{3}$$

where, $\delta = E_p / E_m$.

where, v_v and v_p are the volume fractions of voids/porosity and nanoparticles in the composite respectively and E_m and E_p is elastic moduli of the matrix and the particle respectively.

3. RESULTS AND DISCUSSION

The stiffness and hardness properties of AA1100/TiB_2 composites are shown in figure 1. The elastic stiffness and knoop hardness were increased with volume fraction of TiB_2. The effect of particle size and voids/porosity were not considered in the Rule of Mixture (ROM) criterion. The present criterion considers adhesion, formation of precipitates, particle size, agglomeration, voids/porosity, obstacles to the dislocation, and the interfacial reaction of the particle/matrix. The experimental results were within the upper and lower limits of the present model.

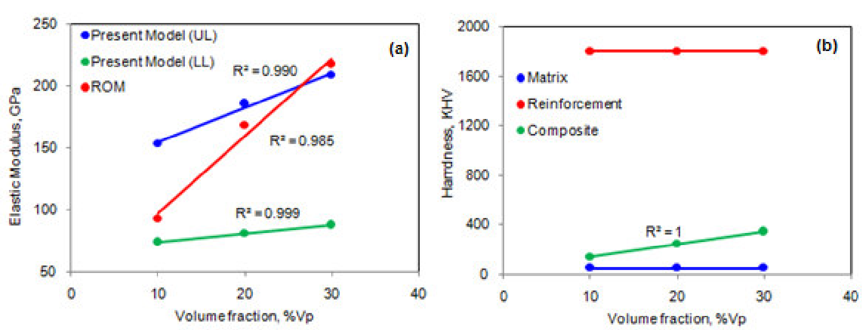

Figure 1: Mechanical Properties of AA1100/TiB_2 composites.

3.1 Effect of volume fraction, Normal Load, Sliding Speed, Sliding distance on Wear Rate

For the analysis of variance (ANOVA), all parameters qualify Fisher's test at 90% confidence level. In Table 3, the percent contribution indicates that the parameter A contributes 43.8% of variation in the wear rate. The normal load (B) adds 21.58% of variation in the wear rate. The speed (C) tenders 15.17% of variation in the wear rate. The sliding distance (D) presents 19.45% of variation in the wear rate. All the parameters are significant in controlling the wear rate of AA1100/TiB_2 composites.

Table 3: ANOVA summary of the effective stress

Source	Sum 1	Sum 2	Sum 3	SS	v	V	F	P
A	19.90000	17.74000	15.91000	2.65940	1	2.6594	1.87E+14	43.8
B	16.34000	18.10000	19.11000	1.31007	1	1.3100667	9.22E+13	21.58
C	18.28000	18.75000	16.52000	0.92127	1	0.9212667	6.48E+13	15.17
D	17.21000	95.88053	53.55000	1.18087	1	1.1808667	8.31E+13	19.45
e				0.00000	4	0.0000	1.00E+00	0
T	71.73000	150.47053	105.09000	6.07160	8			100

Note: SS is the sum of square, v is the degrees of freedom, V is the variance, F is the Fisher's ratio, P is the percentage of contribution and T is the sum squares due to total variation.

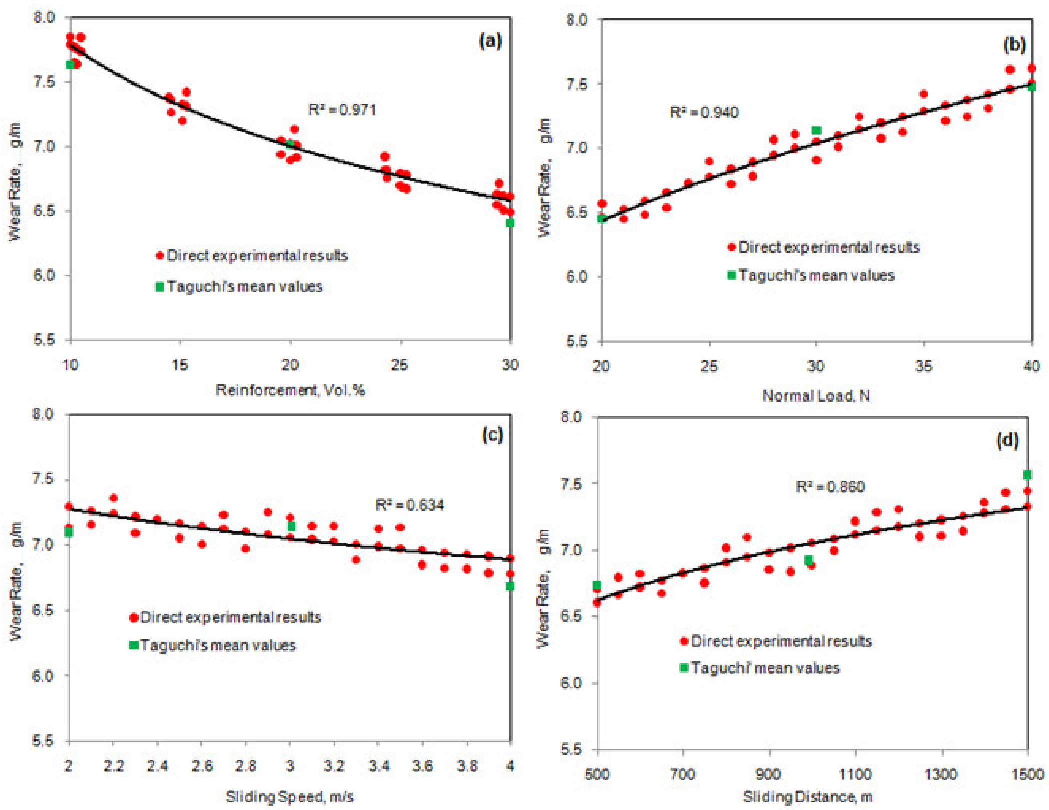

Figure 2: Influence of process parameters on wear rate.

The wear rate was decreased with increase in volume fraction of TiB_2 in AA1100 alloy matrix (figure 2a). This is owing to high hardness of TiB_2 as compared to soft AA1100 alloy matrix. The wear rate was increased with load regardless of composition of the composites as shown in figure 2b. The wear rate was decreased with increase of sliding speed (figure 2c). Increasing the sliding speed made it increasingly difficult for surface damage by plastic deformation. From figure 2d it is observed that the wear rate was increased with the sliding distance. As the sliding distance increases the time of contact between the surfaces were also increased. Hence more volume loss will be there. The mathematical relations between wear and volume fraction of reinforcement, normal load, sliding speed and sliding distance are given by

$$W_{rp} = 5.817 \times {v_f}^{-0.11} \quad (4)$$

$$W_{rf} = 5.042 \times F^{0.104} \quad (5)$$

$$W_{rn} = 7.37 \times N^{-0.01} \quad (6)$$

$$W_{rd} = 5.769 \times d^{0.032} \quad (7)$$

where,
W_{rp} is the wear rate due to vol.% of reinforcement (v_f), g/m
W_{rf} is the wear rate due to normal load (F), g/m
W_{rn} is the wear rate due to speed (N), g/m
W_{rd} is the wear rate sliding distance (d), g/m.

The R-squared values, which are attributable to volume fraction of reinforcement, normal load, sliding speed and sliding distance, are 0.971, 0.940, 0.634 and 0.860, respectively. This trend is similar to the percent contributions of process parameters obtained from Taguchi techniques. The mean values obtained by the Taguchi techniques are within the range of curve fitting as seen in figure 3. Therefore, R-squared values represent not only the fitness of curve but also the strength of process variables. The accuracy of these models depends on the magnitude of penetration during wear tests. The wear depth was correlated with power-law relationship better than the linear one [30].

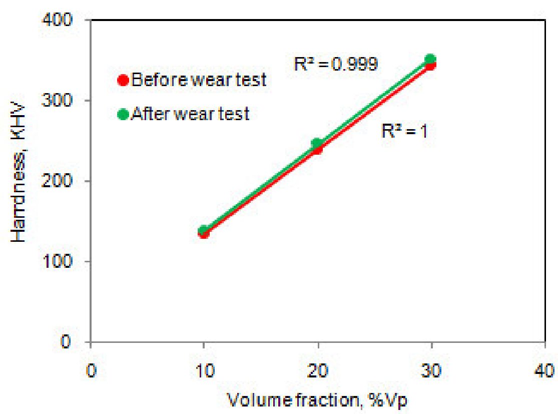

Figure 3: Harness of AA1100/ TiB_2 composites after wear test.

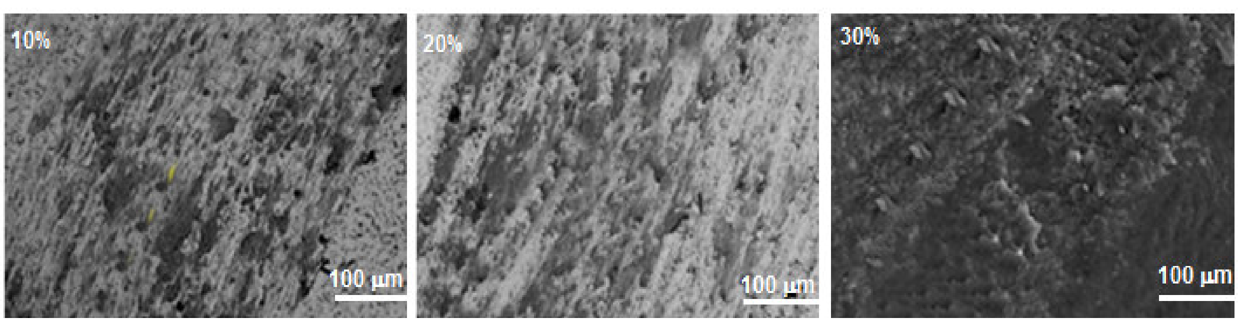

Figure 4: Images of worn surfaces of AA1100/TiB_2 composites: (a) 10 vol.% TiB_2 (b) 20 vol.% TiB_2 and (c) 30 vol.% TiB_2.

3.2 Consequence of Wear in AA1100/TiB_2 Composites

The amount of metal loss depends upon the strength of the variables. It is necessary to distinguish the consequence of wear in AA1100/TiB_2 composites. The hardness values increase after wear test as shown in figure 3. The increase in hardness in the worn specimens may be attributed to the strain hardening mainly due to influence of volume fraction of TiB_2. The microstructures of worn specimens are revealed in figure 4. In the composites having 10% TiB_2, adhesive wear was found between surfaces during frictional contact and unwanted displacement and attachment of wear debris and matrix material from pin surface to disc surface due to plastic deformation. Abrasive wear was occurred in case of composites having 20% 0r 30%TiB_2. The common analogy is that of material being removed or displaced by a plowing operation. When the reinforcement increased from 10 to 30 vol.% the scratches were also increased due to dragging of detached TiB_2 nanoparticles on the surface.

3. CONCLUSION

The mathematical models established in the present work can predict the same kind of trend as estimated by the Taguchi's design of experiments. The abrasive wear was predominant in the composites having high volume fraction of TiB_2.

REFERENCES

1. A. C. Reddy, Mechanical properties and fracture behavior of 6061/SiCp Metal Matrix Composites Fabricated by Low Pressure Die Casting Process, Journal of Manufacturing Technology Research, 1, 2009, pp.273-286.
2. A. C. Reddy, Tensile properties and fracture behavior of 6063/SiC_P metal matrix composites fabricated by investment casting process, International Journal of Mechanical Engineering and Materials Sciences, 3, 2010, pp.73-78.
3. A. C. Reddy and B. Kotiveerachari, Effect of aging condition on structure and the properties of Al-alloy / SiC composite, International Journal of Engineering and Technology, 2, 2010, pp.462-465.
4. A. C. Reddy and B. Kotiveerachari, Influence of microstructural changes caused by ageing on wear behaviour of Al6061/SiC composites, Journal of Metallurgy & Materials Science, 53, 2011, pp. 31-39.
5. A. C. Reddy, Tensile fracture behavior of 7072/SiCp metal matrix composites fabricated by gravity die casting process, Materials Technology: Advanced Performance Materials, 26, 2011, pp. 257-262.
6. A. C. Reddy, Influence of strain rate and temperature on superplastic behavior of sinter forged Al6061/SiC metal matrix composites, International Journal of Engineering Research & Technology, 4, 2011, pp.189-198.
7. A. C. Reddy, Evaluation of mechanical behavior of Al-alloy/SiC metal matrix composites with respect to their constituents using Taguchi techniques, i-manager's Journal of Mechanical Engineering, 1, 2011, pp.31-41.
8. A. Chennakesava Reddy and Essa Zitoun, Matrix al-alloys for alumina particle reinforced metal matrix composites, Indian Foundry Journal, 55, 2009, pp.12-16.
9. A. C. Reddy and Essa Zitoun, Tensile behavior of 6063/Al_2O_3 particulate metal matrix composites fabricated by investment casting process, International Journal of Applied Engineering Research, 1, 2010, pp.542-552.
10. A. C. Reddy and Essa Zitoun, Tensile properties and fracture behavior of 6061/Al_2O_3 metal matrix composites fabricated by low pressure die casting process, International Journal of Materials Sciences, 6, 2011, pp.147-157.
11. A. C. Reddy, Strengthening mechanisms and fracture behavior of 7072Al/Al_2O_3 metal matrix composites, International Journal of Engineering Science and Technology, 3, 2011, pp.6090-6100.
12. A. C. Reddy, Evaluation of mechanical behavior of Al-alloy/Al_2O_3 metal matrix composites with respect to their constituents using Taguchi, International Journal of Emerging Technologies and Applications in Engineering Technology and Sciences, 4, 2011, pp. 26-30.
13. A. C. Reddy, Sliding Wear and Micromechanical Behavior of AA1100/Titanium Oxide Metal Matrix Composites Cast by Bottom-Up Pouring, 7th International Conference on Composite Materials and Characterization, Bangalore, 11-12 December 2009, 205-210.
14. Y. S. A. Kumar, A. C. Reddy, Interfacial Criterion for Debonding of Titanium Boride/AA4015 Metal Matrix Composites, 2nd International Conference on Modern Materials and Manufacturing, Pune, 10-11 December 2010, pp. 265-268
15. Y. S. A. Kumar, A. C. Reddy, Fabrication and Properties of AA7020-TiN Composites under Combined Loading of Temperature and Tension, 2nd International Conference on Modern Materials and Manufacturing, Pune, 10-11 December 2010, pp. 276-280
16. A. C. Reddy, Fracture behavior of brittle matrix and alumina trihydrate particulate composites, Indian Journal of Engineering & Materials Sciences, 9, 2002, pp.365-368.
17. R. G. Math, A. Chennakesava Reddy, Sliding Wear of AA7020/MgO Composites against En32 Steel Disc, 2nd International Conference on Modern Materials and Manufacturing, Pune, 10-11 December 2010, pp. 281-286
18. G. V. R. Kumar, A. Chennakesava Reddy, Tribological Analogy of Cast AA2024/TiB2 Composites, 2nd International Conference on Modern Materials and Manufacturing , Pune, 10-11 December 2010, 287-291
19. A. C. Reddy, Wear and Mechanical Behavior of Bottom-Up Poured AA4015/Graphite Particle-Reinforced Metal Matrix Composites, 6th National Conference on Materials and Manufacturing Processes, Hyderabad, 8-9 August 2008, pp. 120-126.
20. A. C. Reddy, S. Sundararajan, Influences of ageing, inclusions and voids on the ductile fracture mechanism of commercial Al-alloys, Journal of Bulletin of Material Sciences, 28, 2005, pp. 75-79.
21. A. C. Reddy, S. Madahava Reddy, Evaluation of dry sliding wear characteristics and consequences of cast Al-Si-Mg-Fe alloys, ICFAI Journal of Mechanical Engineering, 3, 2010, pp.1-13.
22. A. C. Reddy, M. Vidya Sagar, Two-dimensional theoretical modeling of anisotropic wear in carbon/epoxy FRP composites: comparison with experimental data, International Journal of Theoretical and Applied Mechanics, 6. 2010, pp. 47-57.
23. J.L. Routbort, R.O. Scattergood and A.P.L. Turner, The erosion of reaction-bonded SiC, Wear, 59, 1980, pp. 363-375.
24. G. Beckmann and J. Gotzmann, Analytical model of the blast wear intensity of metals based on a general arrangement for abrasive wear, Wear, 73, 1981, pp. 325-353.
25. J.H. Williams Jr. and E.K. Lau, Solid particle erosion of graphite-epoxy composites, Wear, 29, 1974. P. 219.

26. A. Chennakesava Reddy, V.M. Shamraj, Reduction of cracks in the cylinder liners choosing right process variables by Taguchi method, Foundry Magazine, 10, 1998, pp. 47-50.
27. A. Chennakesava Reddy, V.S.R. Murti, S. Sundararajan, Control factor design of investment shell mould from coal flyash by Taguchi method, Indian Foundry Journal, 45, 1999, pp. 93-98.
28. S. Tsuchitani, R. kaneko, S. Hirono, Effects of humidity on nanometer scale wear of a carbon film, Tribology International, 40, 2007, pp. 306-312.